Journal of Magnetism and Magnetic Materials 528 (2021) 167803

Contents lists available at ScienceDirect

Journal of Magnetism and Magnetic Materials

journal homepage: www.elsevier.com/locate/jmmm

Research articles

Optical and magneto-optical properties of epitaxial Mn_2GaC MAX phase thin film

Sergey Lyaschenko [a,*], Olga Maximova [a,b,*], Dmitriy Shevtsov [a], Sergey Varnakov [a], Ivan Tarasov [a], Ulf Wiedwald [c], Johanna Rosen [d], Sergei Ovchinnikov [a,b], Michael Farle [a,c]

[a] Kirensky Institute of Physics, Federal Research Center KSC SB RAS, Krasnoyarsk 660036 Russia
[b] Siberian Federal University, 660041 Krasnoyarsk, Russia
[c] Faculty of Physics, University of Duisburg-Essen, 47057 Duisburg, Germany
[d] Thin Film Physics Division, Department of Physics, Chemistry and Biology (IFM), Linköping University, SE-581 83 Linköping, Sweden

ARTICLE INFO

Keywords:
MAX phases
Magnetism
Epitaxial thin films
Spectral magneto-ellipsometry
Magnetic circular dichroism

ABSTRACT

We report measurements of the dielectric permittivity, optical conductivity and magnetic circular dichroism (MCD) of the epitaxial Mn_2GaC MAX-phase thin film in an external magnetic field of up to 200 mT, at temperatures of 296 and 140 K and 1.4 to 3.5 eV. The optical conductivity and MCD spectra show absorption peaks which are consistent with the interband electronic transitions for different positions of Mn, Ga, and C ions as confirmed by theoretical calculations of the spin-dependent density of electronic states. The well-known structural phase transition at 214 K is also seen in the changes of optical, magneto-optical and surface magnetic properties of Mn_2GaC in our experiment.

1. Introduction

In the last decade, research interest in layered hexagonal $M_{n+1}AX_n$ structures (also abbreviated MAX materials) has noticeably increased: where n - takes integer values 1, 2 and 3. M is an early transition element (e.g., Sc, Ti, V, Cr, Zr, Nb, Mo, Hf, Ta). A is an element from group 13 or 14 (for example, Al, Si, P, S, Ga, Ge, As, Cd, In, Sn, Tl, Pb), X is C or N [1–3]. Barsoum and El-Raghy reported in 1996 a striking combination of the properties of metals and ceramics for the Ti_3SiC_2 compound and further demonstrated these properties are common to the entire family of MAX materials [4]. Further extension from the basic ternary compounds to various structural combinations of M-elements and C-N mixtures at the X position [5] is of interest, which ultimately yields several hundred different MAX phases [6] with a high chemical resistance to aggressive media, high thermal stability, mechanical strength and strong anisotropy of the electronic properties. For practical applications they are found in high-temperature ceramics [7], catalysts, protective coatings, and thermoelectric converters [8–10]. Since the $M_{n+1}Xn$ layers alternate with the layers of A atoms and have weaker chemical bonds with them, MAX phases are used as parent material in the synthesis of 2D MXenes structures which are promising for the creation of energy storage and conversion devices, coatings, and filters [11,12].

In addition to the interest in the structural and electronic properties of the MAX materials, interest in their magnetic properties is also significant. The magnetic phenomena in combination with the atomic-layered structure and the proposed tunable anisotropic transport properties [13] could yield functional materials for various applications in spintronics. Furthermore they are ideal systems for basic research of complex magnetic phenomena. The early transition metals in the M elements do not form the MAX phase with room-temperature ferromagnetic behavior [14]. Therefore, it is necessary to expand the family of M elements to fully realize the potential of these nanolaminate compounds in spintronics. The key for controlling a complex magnetic behavior is the ability to manipulate magnetic interactions [15,16]. In this regard, compounds containing Mn are of interest which exhibit magnetic and structural transitions as a function of temperature [17–21].

The magnetic Mn_2GaC MAX-phase was theoretically predicted and subsequently synthesized as a heteroepitaxial thin film on the MgO (1 1 1) substrate [14]. This compound may be considered as an ideal model system for studying complex magnetic phenomena occurring in atomic-layered materials [22]. $Mn_2GaC(0001)/MgO(1\,1\,1)$ has a hexagonal three-layer structure belonging to the space group P63/mmc with a primitive unit cell represented by 8 atoms, i.e. 4 Mn, 2 Ga and 2C,

* Corresponding authors at: Kirensky Institute of Physics, Federal Research Center KSC SB RAS, Akademgorodok 50, bld. 38, Krasnoyarsk, 660036, Russia.
E-mail addresses: lsa@iph.krasn.ru (S. Lyaschenko), maximo.a@mail.ru (O. Maximova).

https://doi.org/10.1016/j.jmmm.2021.167803
Received 21 October 2020; Received in revised form 24 December 2020; Accepted 25 January 2021
Available online 30 January 2021

consisting of Mn-C-Mn (Mn_2C) planes alternating with Ga atomic layers [23]. Atomic layers are stacked along the c axis resulting in a strong anisotropy of thermal and electronic as well as magnetic properties. Studies of the structural, magnetic, magnetotransport, magnetostrictive, and magnetocaloric properties of the Mn_2GaC(0001)/MgO (1 1 1) heterostructure [23] showed that the Néel temperature in Mn_2GaC is about 507 K, at which the system changes from the antiferromagnetic (AFM) state to the paramagnetic state. The Mn_2GaC MAX-phase undergoes a first-order phase transition from the AFM collinear to the AFM noncollinear spin state below 214 K. Both states exhibit a large uniaxial magnetostriction along the c axis which results from the magneto-structural transformation into a ferromagnetic (FM) state induced by a strong magnetic field. However, according to the magnetometry the Mn_2GaC(0001)/MgO(1 1 1) sample exhibits a remanent magnetization at 300 K.

Mn_2GaC shows the ferrimagnetic properties at room temperature and in weak magnetic fields due to the AFM non-collinear alignment of magnetic moments in adjacent Mn_2C layers separated by Ga. A reasonable compromise for the magnetic structure based on the observed AFM alignment by neutron reflectometry and the FM component from magnetometry is a canted AFM configuration [24]. A canted AFM structure means that the magnetic moments of the Mn_2C slabs across the Ga layers are not collinear and the angle between AFM coupled moments is below 180°. It could be attributed to the diffusion of carbon atoms into Ga layer and possible surface oxidation layer of Mn_2C [25]. All these phenomena may introduce significant perturbations into the electronic structure of the Mn_2GaC compound.

It was previously shown [26] the nonequivalent states of Mn and Ga ions are present in the Mn_2GaC unit cell. These should be detectable in optical absorption and MCD spectra due to the modification of electronic and magnetic properties, because the above methods lead to the experimental determination of parameters that are somehow associated with magnetic moments on the molecular scale. From temperature dependent changes of the MCD spectra, it is possible to obtain information on the type of ions participating in ferrimagnetic ordering at high temperatures [27,28]. Therefore, this work aims to measure the optical properties of the Mn_2GaC(0001)/MgO(1 1 1) film and the spectral dependences of MCD by reflection magneto-ellipsometry, spectral ellipsometry and transverse magneto-optical Kerr effect at different temperatures in the spectral region 1.4–3.5 eV.

2. Experiment

In this work we studied a 100 nm thick Mn_2GaC(0001) epitaxial thin film grown on a MgO(1 1 1) substrate. The thin film was deposited by magnetron sputter epitaxy (MSE) using three confocal sources with elemental targets: carbon (99.99% purity), manganese (99.95%) and gallium (99.99995% purity). The base pressure in the process chamber was $<5{\cdot}10^{-7}$ Pa, and during the deposition, an argon pressure of 0.455 Pa was used to operate the magnetron. For 60 min before the deposition and during the deposition process, the temperature of the substrate was 550 °C. Details of the synthesis is discussed elsewhere [14,29,30]. The phase composition was confirmed by X-ray diffraction (XRD) using a Panalytical Empyrean MRD system equipped with a Cu-K_α source. Fig. 1 shows X-ray diffraction of the Mn_2GaC epitaxial thin film grown on MgO (1 1 1). Only reflections originating from the film corresponding to the texturing on plane (1 1 1) of the substrate MgO are observed. Furthermore, the lattice parameter c obtained from XRD are 12.54 ± 0.01 Å, respectively, compared with 12.49 Å for the calculated AFM$[0001]_2^A$ spin configuration [14].

Spectral ellipsometric (Ψ, Δ) and magneto-ellipsometric (δΨ, δΔ) measurements of the Mn_2GaC film were performed on a spectral ellipsometer Ellipse-1891 (ISP SB RAS) with a dipole electromagnet and a 150 W Xe lamp (Hamamatsu) as a light source [31]. The sample was placed in a specially-made high-vacuum austenitic stainless-steel

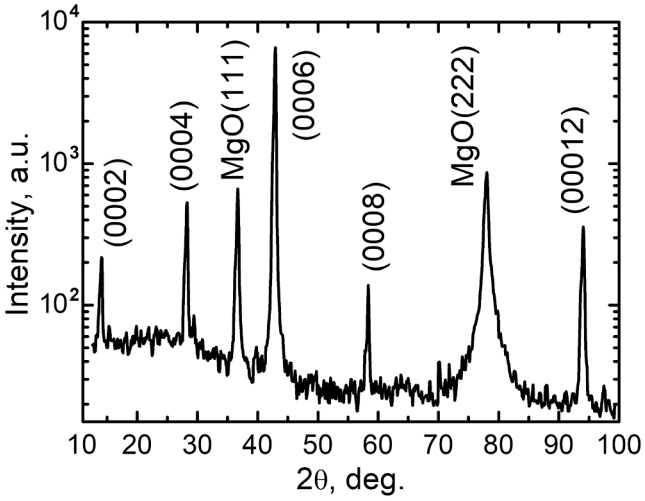

Fig. 1. XRD scan of the epitaxial Mn_2GaC film on MgO(1 1 1) substrate.

cryostat with a copper holder and fused silica optical windows. Before the measurements, the sample was heated in the cryostat in a vacuum of 10^{-4} Pa for 15 h at a temperature of 105 °C. All ellipsometric and magneto-ellipsometric measurements were carried out between room temperature and 140 K.

The ellipsometric spectra were recorded from 370 to 900 nm. The angle of incidence of light φ_0 was set at 60° to the normal of the sample. Field dependent magneto-optical measurements were carried out in a quasi-static magnetic field of up to 75 mT in white light using an SZS-9 broadband filter. The SZS-9 filter has a wide transmission peak from 360 to 580 nm, with a maximum at 475 nm (2.61 eV). The transmittance peak matches the region of the spectrum with small experimental errors in magneto-ellipsometry. The magnetization reversal loops were measured by the amplitude of the Ψ ellipsometric parameter [32] which is proportional to the imaginary part (ellipticity) of the magneto-optical Kerr effect. Spectral magneto-ellipsometric measurements were carried out in remagnetizing fields of ±200 mT. The details of the spectral magneto-ellipsometric measurement algorithm are presented in [33]. The magnetic field in our measurements was always parallel to the film surface and perpendicular to the plane of incidence of light.

To calculate all components of dielectric permittivity tensor ε of the Mn_2GaC film from the ellipsometric (Ψ, Δ) and magneto-ellipsometric (δΨ, δΔ) data, we used the model of a homogeneous semi-infinite medium and took the magneto-optical contribution to ellipsometric relations as small disturbances into account [34]. The diagonal ε_{11} and off-diagonal ε_{12} components of the ε tensor were calculated as follows [35]:

$$\varepsilon_{11} = \sin(\varphi_0)^2 \cdot \left(\tan(\varphi_0)^2 \cdot \left(\frac{1-\rho}{1+\rho} \right)^2 + 1 \right), \quad \rho \equiv \tan(\Psi) \cdot exp(i \cdot \Delta) \tag{1}$$

$$\varepsilon_{11} = Re(\varepsilon_{11}) - i \cdot Im(\varepsilon_{11}) = (n - i \cdot k)^2 \tag{2}$$

$$\varepsilon_{12} = Re(\varepsilon_{12}) - i \cdot Im(\varepsilon_{12}) = = -i \cdot (Re(\varepsilon_{11}) - i \cdot Im(\varepsilon_{11}))(Q_1 - i \cdot Q_2) \tag{3}$$

where n is the refractive index, k is the extinction coefficient, $Q = Q_1 - iQ_2$ is the magneto-optical parameter.

The magneto-optical parameter Q, which is used in (3), was determined from Ψ, Δ, δΨ, and δΔ which are measured by means of magneto-optical ellipsometry. The experimental error of Q was calculated by the law of error propagation [36]. Similarly, the errors of ε components and the magnitude of the magnetic circular dichroism (MCD) were obtained. The calculated spectral dependences n, k, and Q were used to determine the magnitude of the MCD using the formula [37] (λ is the wavelength):

$$MCD = -\frac{\pi}{\lambda} Im((n - i\cdot k)\cdot Q) \quad (4)$$

The model of a homogeneous semi-infinite medium was chosen due to the following reasons:

1) a sufficiently large film thickness in comparison with the skin depth of light;

2) the lack of information on the thickness and optical properties of a possible oxide layer on the surface of Mn_2GaC;

3) the opacity of the Mn_2GaC film in the spectral range of 270–900 nm.

3. Results and discussion

The field dependences of Ψ on the Mn_2GaC(0001)/MgO(1 1 1) sample are shown in Fig. 2. The loops are shifted in one direction by 250 Oe at 140 K and by approximately 130 Oe at room temperature. At 140 K, there is hysteresis with a coercive force at about 250 Oe. The possible reason for the asymmetry of magneto-optical loops is the exchange bias in the sample structure [38], as a result of interaction between the FM sublayers and the AFM-ordered bulk structure. It should be noted that the measured field dependences are likely to characterize mainly the magneto-optical properties of the sample surface layer due to the exponential attenuation of light with depth and the absence of reflection from the substrate (details on Fig. 5) [35,39]. Therefore, the observed parameters of the loops can be caused by magnetizing effects in the surface layer of the sample, the contribution of which is insignificant in the case of SQUID measurements and vibration magnetometry.

The amplitude of the ellipsometric signal at 140 K and 296 K cannot be considered as proportional to the magnetization of the sample because of the dependence of the optical and magneto-optical properties of the sample on the temperature and energy of the light. For example, there is nearly no temperature dependence of the phase δΔ in the spectral range 1.7–2.9 eV in contrast to the amplitude parameter Ψ (Fig. 3).

The spectra of the diagonal and off-diagonal components of the dielectric permittivity of the Mn_2GaC film are shown in Fig. 4 in comparison with similar data for a ferromagnetic polycrystalline iron film. The real part of the dielectric permittivity of the film has a strong temperature dependence, which is expressed in a significant increase in the extinction coefficient (Fig. 5) when the sample is cooled down to 140 K. Such dependence on temperature is typical for metals.

A comparison of ε_{12} spectra with similar data of a ferromagnetic Fe film (Fig. 4) from [34] shows a ten times weaker magneto-optical activity in the visible light range for Mn_2GaC even at low temperature. A

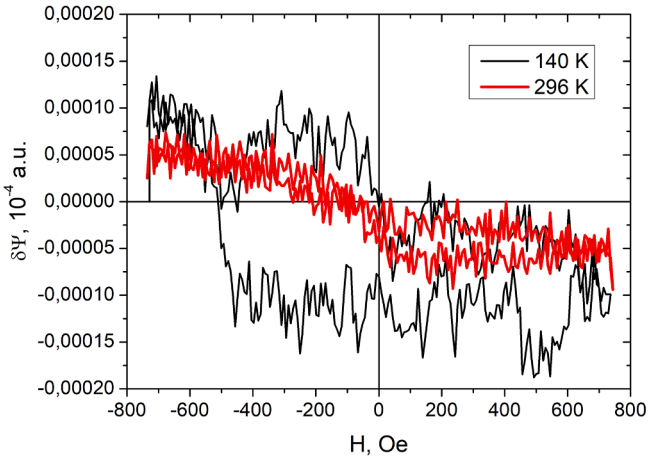

Fig. 2. Magnetic field hysteresis of ellipsometric data at different temperatures (after subtracting the baselines) in energy range from 2.13 to 3.44 eV with a maximum at 2.61 eV.

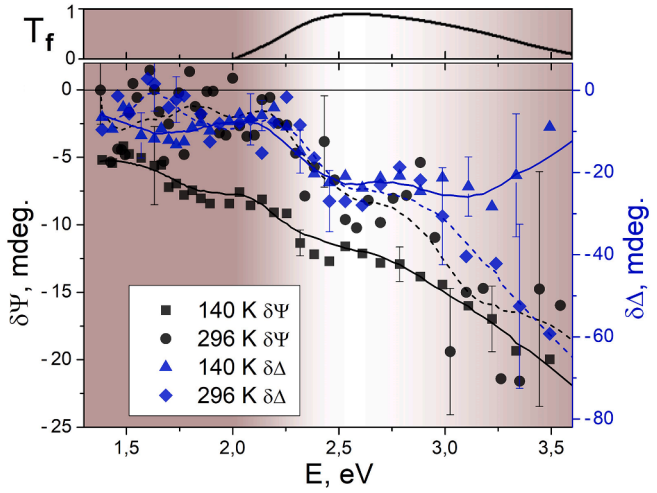

Fig. 3. Spectral dependences of the magneto-ellipsometric amplitude and phase at 140 K and 296 K. The top inset shows the spectrum of normalized light transmision T_f of optical filter SZS-9.

zero-crossing of $Im(\varepsilon_{12})$ is not observed in the MAX phase. The difference in sign of $Re(\varepsilon_{11})$ between Fe and Mn_2GaC is a consequence of differences in n_2-k_2 values for both materials and shows a greater influence of optical absorption in epitaxial Mn_2GaC in comparison with a polycrystalline Fe film.

To understand in detail the temperature changes in the optical properties, the optical conductivity of the Mn_2GaC film was calculated using the formula $\sigma = Im(\varepsilon_{11})\omega/4\pi$, where ω is the frequency of the optical wave. Fig. 6a shows the spectra of σ at different temperatures, and Fig. 6b shows absolute changes $\Delta\sigma = \sigma_{140\ K} - \sigma_{296\ K}$, respectively.

Optical conductivity spectra allow us analyzing electronic transitions independently from spin orientation. As it can be seen from the σ spectra, there are no significant changes in the optical absorption during sample cooling in the near-infrared range up to 1.9 eV. Changes of 1.46 eV can be caused by hardware noise. The most visible changes are observed in the range from 2 to 3.5 eV. The changes of two peaks at 2.44 eV and 3.36 eV and a small change of two peaks at 2.77 eV and 3.00 eV are pronounced.

Significant variations in the electronic transitions under cooling are due to changes occurred in the electronic structure of Mn_2GaC below 214 K. Namely, the enhancement of interband transitions in the Mn-Ga-Mn system may be caused by the lattice contraction [22,23].

To understand which spin-dependent electronic transitions in Mn_2GaC determine the ferrimagnetic response at temperatures above 214 K the MCD spectrum was calculated at 140 and 296 K from the measured off-diagonal components ε_{12} of the dielectric permittivity tensor ε of the sample [37]. For the optimal and demonstrative decomposition of MCD spectra into absorption peaks, calculations with a different number of fitting Gaussian m were performed. Table 1 shows the values of the standard deviation $S = \sqrt{\frac{1}{p}\sum_{j=1}^{p}\left(\left\langle y_j\right\rangle - f(x_j)\right)^2}$ as a function of the number of Gaussian curves m at the approximation of MCD spectra for 140 and 296 K, where p is the number of experimental points, $<y_j>$ and f_j is the experimental value of MCD and the sum of all Gaussian curves at point j, respectively. The calculation of the S value was performed for the region 1.45–3.5 eV.

From Table 1 we can see that as the number of Gaussian peaks m grows, the value of S decreases. For m being less than four, the addition of each successive Gaussian sharply reduced the deviation of S. However, with the approximation of the experimental curve by four or more peaks, further changes of S are insignificant. Both the results of the MCD calculation and spectra decomposition into a series of four Gaussian peaks are presented in Fig. 7.

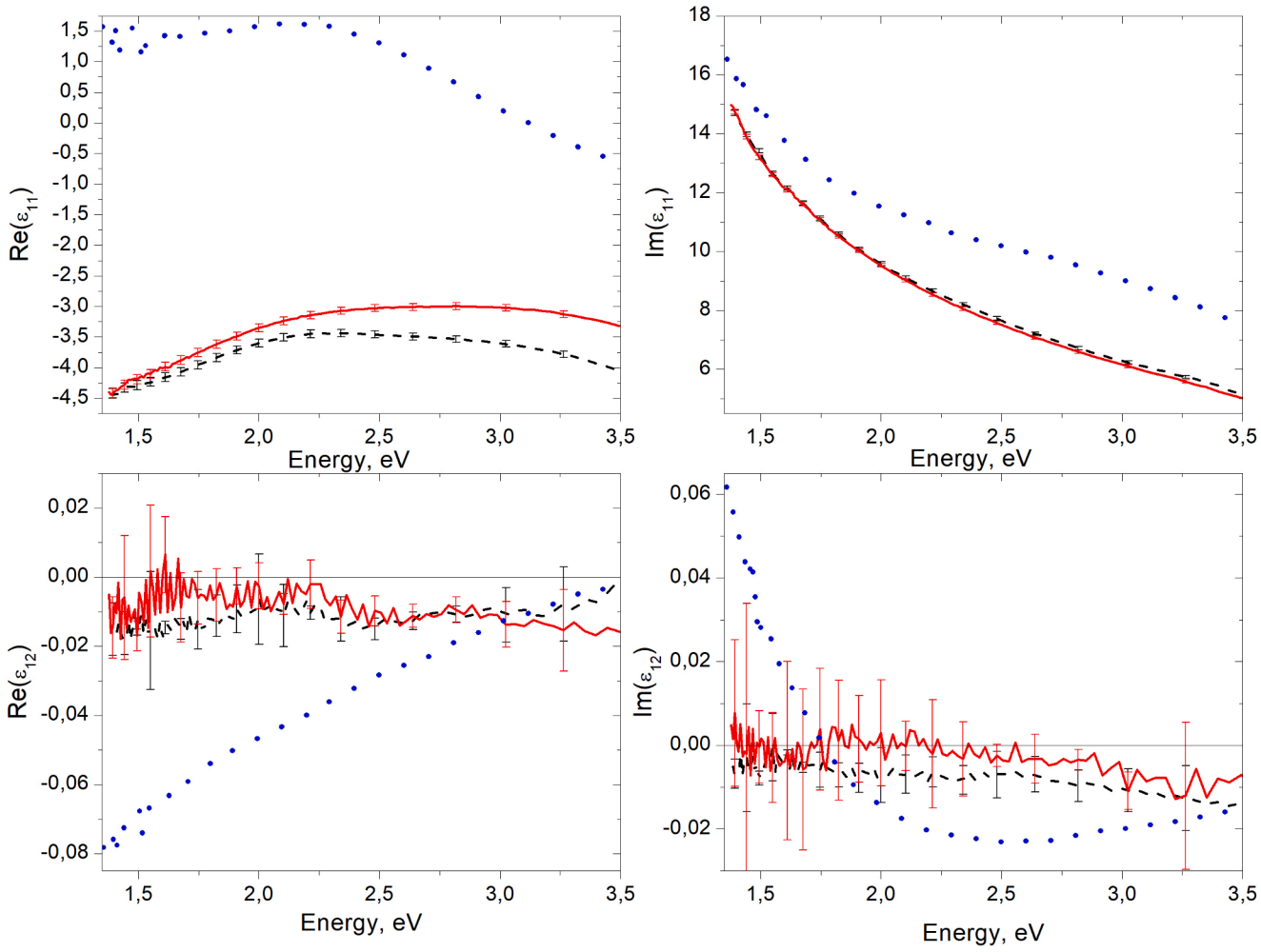

Fig. 4. Spectral dependences of the diagonal and off-diagonal components of ε tensor at different temperatures: dashed black lines – Mn_2GaC sample at 140 K, solid red lines – Mn_2GaC sample at 296 K. Dotted blue lines: 160 nm Fe-film at 296 K from [34] (the values of Re(ε_{12}) and Im(ε_{12}) are divided by 7).

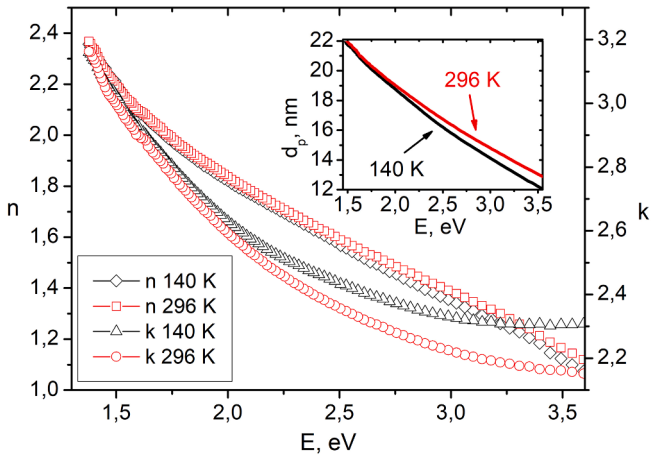

Fig. 5. Refractive index n and extinction coefficient k of Mn_2GaC at different temperatures. The inset shows the spectrum of light penetration depth $d_p = \lambda/(4\pi k)$ by equation (2.37) from [35].

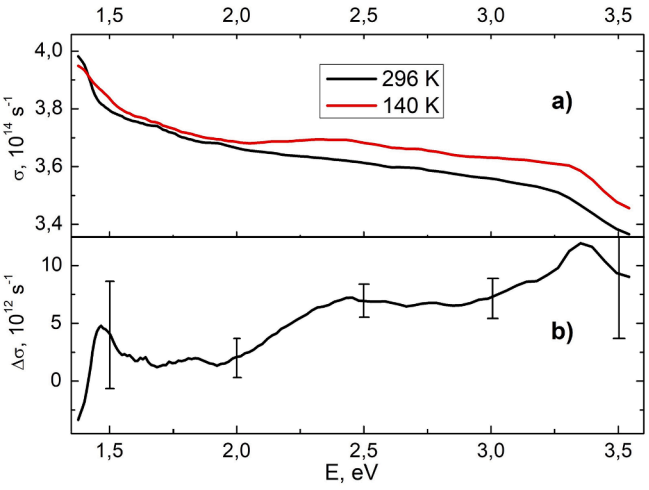

Fig. 6. Mn_2GaC optical conductivity changes at different temperatures.

A series of maxima can be identified in the spectra despite the large experimental noise. Only the peaks which contribute most to the form of the experimental spectrum were considered. Spectral areas less than 2 eV and more than 3.5 eV contain high hardware noise due to the peculiarities of the optical circuit. All this makes it impossible to estimate reliably the temperature changes of peaks 1 and 4 in both spectra. However, the central regions of both curves clearly show the correspondence between each other.

During heating the positions of the maxima of all the peaks shift. These shifts are possibly caused by low signal/noise value.

Table 1
Deviation S for MCD spectra vs the number m of involved Gaussian curves.

m	$S_{140\ K}$, 10^{-6} nm^{-1}	$S_{296\ K}$, 10^{-6} nm^{-1}
1	1.32	3.08
2	1.09	2.29
3	0.59	1.29
4	0.50	0.99
5	0.35	0.88
6	0.26	0.79

Magnetostriction effects which are observed in much larger fields [23] are not considered. The intensity of all resonances, except peak 4, strongly decreases as the sample is heated. The smallest relative changes are observed for peaks 2 and 4. Peak 1 and a weak peak at around 2.9 eV at 140 K, which was not taken into account during decomposition, almost disappear. Peak 3 at 2.53–2.56 eV strongly decreases.

In the following we discuss density functional theory (DFT) calculations of the spin-dependent density of electronic states of Mn_2GaC for understanding the observed changes in the interband transitions. A. Thore et al. have calculated the electronic band structure and total and partial density of states for ferromagnetic and antiferromagnetic states, with distinct FM layers of Mn_1 and Mn_2 in a AFM$[0001]_4^A$ configuration, the latter corresponding to 4 consecutive Mn layers with the same spin orientation before changing sign upon crossing a Ga layer [26]. For this AFM phase the total DOS for spin-up and spin-down states are equal, while the partial density of states (PDOS) for the FM layers Mn_1 and Mn_2 are spin polarized (Fig. 8).

Table 2 shows the numerical correlation between the interband transitions from the PDOS and the observed MCD absorption peaks. The PDOS data are shown by the energy values for the density maxima. But for each such maximum the base width is about 0.2 eV, which as a result of summation can show a broad peak for MCD. Additional broadening of the MCD peaks can also result from the presence of many satellite density maxima from the DFT calculation.

According to the density of states and the diagram of atomic positions in the Mn_2GaC cell [26], it can be seen that the main contribution to the absorption peaks is made by transitions in Mn_1 and Mn_2 ions, as well as transitions between Mn_2 - Ga_2 and Mn_1 - Ga_1. The bound states of Mn and C at −3.5 eV give transition energies outside the spectral range in which we conduct the measurements. Thus, for MCD, it is possible to associate the measured spectra with possible prominent interband transitions according to the PDOS corresponded to Mn_2GaC in AFM $[0001]_4^A$ state.

Significant attenuation of the intensities of peaks 1, 3, and the weak peak at around 2.9 eV can be explained by the weakening of the interaction of external electronic levels between ions $Mn_2 - Ga_2$ and $Mn_{1,2} - C$ which is caused by the lattice stretching above the phase transition.

4. Conclusion

Usually in the ex-situ measurements the material surface is oxidized. As ellipsometry is particularly useful to determine the layer thickness, the reflectivity data may be used to estimate the thickness of oxidation, evaluate the possible contribution to hysteresis loop and MCD data. However, such analysis requires a special design of the technological chamber. Spectral in-situ magneto-ellipsometry measurements are required before and after the interaction of the sample with oxygen without changing the geometrical position of the sample in the optical scheme. We plan to provide such research in future.

In summary, we have studied the optical and magneto-optical properties of a 100 nm Mn_2GaC epitaxial film in magnetic fields up to 200 mT between 296 and 140 K around the structural phase transition temperature of 214 K. The abrupt lattice expansion of the Mn-C-Mn layers leads to significant change in the spectral optical properties. Our findings are consistent with the assumption that Ga affects the interband electronic transitions in Mn and C and non-collinear

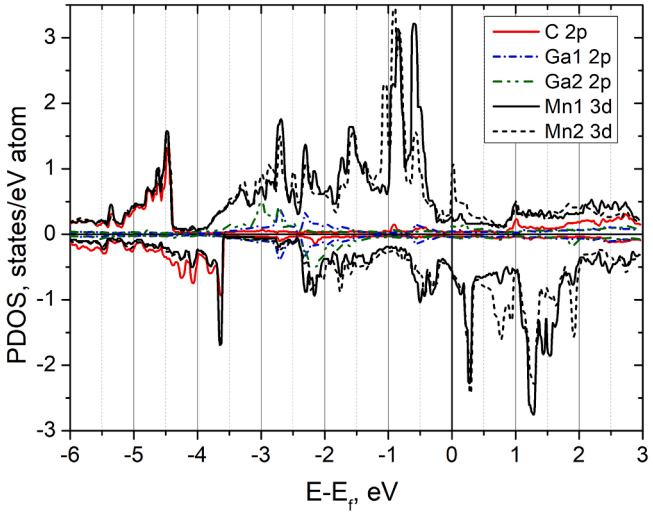

Fig. 8. PDOS from [26] at 0 K for FM layers Mn_1 and Mn_2 in AFM $[0001]_4^A$ Mn_2GaC. Positive states – spin-up ↑, negative states – spin-down ↓.

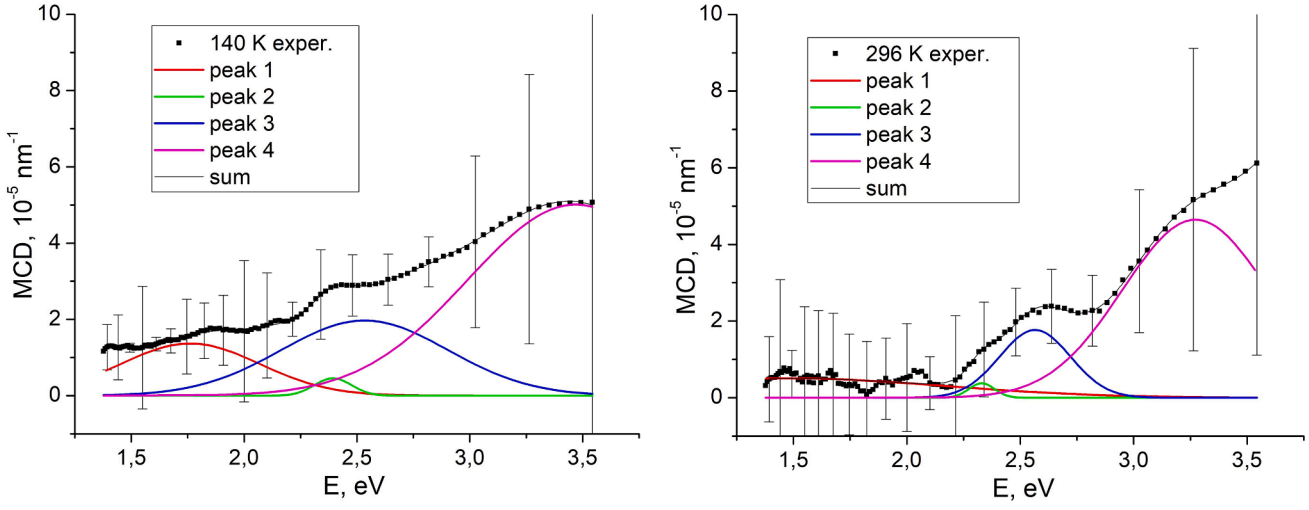

Fig. 7. MCD results for Mn_2GaC from magneto-ellipsometric measurements at 140 and 296 K.

Table 2
Interband transitions associated with the peaks observed on the MCD spectra for the epitaxial Mn_2GaC film.

Peak 1 (1.47–1.76 eV)
$Mn_{1,2}\uparrow$ (−1.6 eV) → $Mn_{1,2}\uparrow$ (+0.2 eV);
$Mn_{1,2}\uparrow$ (−0.6 eV) → $Mn_{1,2}$&C↑ (+1 eV);
$Mn_{1,2}\downarrow$ (−0.5 eV) → $Mn_{1,2}\downarrow$ (+1.3 eV).
Peak 2 (2.33–2.39 eV)
$Mn_{1,2}\uparrow$ (−2.2 eV) → $Mn_{1,2}\uparrow$ (+0.2 eV);
$Mn_{1,2}\uparrow$ (−1.4 eV) → $Mn_{1,2}$&C↑ (+1 eV);
$Mn_2\downarrow$ (−0.5 eV) → $Mn_2\downarrow$ (+1.9 eV);
$Mn_2\downarrow$ (−1.6 eV) → $Mn_2\downarrow$ (+0.8 eV).
Peak 3 (2.53–2.56 eV)
$Mn_{1,2}\uparrow$ (−2.3 eV) → $Mn_{1,2}\uparrow$ (+0.2 eV);
$Mn_{1,2}\uparrow$ (−1.6 eV) → $Mn_{1,2}$&C↑ (+1 eV);
$Mn_{1,2}\uparrow$ (−0.6 eV) → $Mn_{1,2}$&C↑ (> +2 eV);
$Mn_{1,2}\downarrow$&Ga2↓ (−2.2 eV) → Mn1,2↓ (+0.3 eV);
$Mn_{1,2}\downarrow$ (−0.6 eV) → $Mn_{1,2}\downarrow$ (+1.8 eV).
Weak peak at 2.9 eV
$Ga_2\downarrow$ (−2.2 eV) → $Mn_2\downarrow$ (+0.7 eV).
Broad peak 4 (3.27–3.46 eV)
$Mn_{1,2}$&Ga2↓ (−2.3 eV) → $Mn_{1,2}\downarrow$ (+1.3 eV)
$Mn_{1,2}$&Ga2↓ (−2.7 eV) → $Mn_{1.2}\downarrow$ (+1.8 eV).

(uncompensated) magnetic moments in alternating Mn-C-Mn layers lead to ferrimagnetic properties at room temperature. Furthermore, we identify a possible contribution of the Mn_2GaC surface to the bulk magnetic properties from the temperature dependence of Kerr hysteresis loops. The experimental MCD spectra are identified as interband transitions in the AFM $[0001]_4^A$ state.

CRediT authorship contribution statement

Sergey Lyaschenko: Methodology, Investigation, Data curation, Software, Formal analysis, Writing - original draft, Visualization, Validation. **Olga Maximova:** Software, Formal analysis, Writing - original draft, Visualization. **Dmitriy Shevtsov:** Investigation, Writing - original draft. **Sergey Varnakov:** Writing - original draft, Supervision, Funding acquisition. **Ivan Tarasov:** Conceptualization, Writing - original draft. **Ulf Wiedwald:** Resources, Investigation. **Johanna Rosen:** Methodology, Writing - review & editing. **Sergei Ovchinnikov:** Resources, Writing - original draft, Supervision, Funding acquisition. **Michael Farle:** Conceptualization, Writing - review & editing, Visualization, Project administration.

Declaration of Competing Interest

The authors declare that they have no known competing financial interests or personal relationships that could have appeared to influence the work reported in this paper.

Acknowledgements

The research was supported by the government of the Russian Federation (agreement No. 075-15-2019-1886) and the Deutsche Forschungsgemeinschaft (DFG, German Research Foundation) – Project-ID 405553726 – TRR 270. We thank Andrejs Petruhins for preparation of the samples. J. R. acknowledges funding from the Swedish Research Council (VR), project 642-2013-8020.

References

[1] M.W. Barsoum, M. Radovic, Elastic and mechanical properties of the MAX phases, Annu. Rev. Mater. Res. 41 (2011) 195–227, https://doi.org/10.1146/annurev-matsci-062910-100448.
[2] Z.M. Sun, Progress in research and development on MAX phases: a family of layered ternary compounds, Int. Mater. Rev. 56 (2011) 143–166, https://doi.org/10.1179/1743280410Y.0000000001.
[3] M.W. Barsoum, The Mn+1AXn phases and their properties, in: R. Riedel and I.-W. Chen (Ed.), Ceram. Sci. Technol., 1st ed., Wiley-VCH Verlag GmbH & Co. KGaA, Weinheim, Germany, 2010: pp. 299–347.
[4] M.W. Barsoum, T. El-Raghy, Synthesis and characterization of a remarkable ceramic: Ti3SiC2, J. Am. Ceram. Soc. 79 (1996) 1953–1956, https://doi.org/10.1111/j.1151-2916.1996.tb08018.x.
[5] A.S. Ingason, A. Mockute, M. Dahlqvist, F. Magnus, S. Olafsson, U.B. Arnalds, et al., Magnetic self-organized atomic laminate from first principles and thin film synthesis, Phys. Rev. Lett. 110 (2013), 195502, https://doi.org/10.1103/PhysRevLett.110.195502.
[6] M. Sokol, V. Natu, S. Kota, M.W. Barsoum, On the chemical diversity of the MAX phases, Trends Chem. 1 (2019) 210–223, https://doi.org/10.1016/j.trechm.2019.02.016.
[7] A.S. Ingason, M. Dahlqvist, J. Rosen, Magnetic MAX phases from theory and experiments; a review, J. Phys. Condens. Matter. 28 (2016), 433003, https://doi.org/10.1088/0953-8984/28/43/433003.
[8] M.W. Barsoum, The MN+1AXN phases: a new class of solids, Prog. Solid State Chem. 28 (2000) 201–281, https://doi.org/10.1016/S0079-6786(00)00006-6.
[9] H. Högberg, L. Hultman, J. Emmerlich, T. Joelsson, P. Eklund, J.M. Molina-Aldareguia, et al., Growth and characterization of MAX-phase thin films, Surf. Coatings Technol. 193 (2005) 6–10, https://doi.org/10.1016/j.surfcoat.2004.08.174.
[10] H.B. Zhang, Y.C. Zhou, Y.W. Bao, J.Y. Wang, Oxidation behavior of bulk Ti 3 SiC 2 at intermediate temperatures in dry air, J. Mater. Res. 21 (2006) 402–408, https://doi.org/10.1557/jmr.2006.0046.
[11] M. Naguib, V.N. Mochalin, M.W. Barsoum, Y. Gogotsi, 25th Anniversary Article: MXenes: A New Family of Two-Dimensional Materials, Adv. Mater. 26 (2014) 992–1005, https://doi.org/10.1002/adma.201304138.
[12] J. Pang, R.G. Mendes, A. Bachmatiuk, L. Zhao, H.Q. Ta, T. Gemming, et al., Applications of 2D MXenes in energy conversion and storage systems, Chem. Soc. Rev. 48 (2019) 72–133, https://doi.org/10.1039/C8CS00324F.
[13] M. Barsoum, T. El-Raghy, The MAX Phases: unique new carbide and nitride materials, Am. Sci. 89 (2001) 334, https://doi.org/10.1511/2001.28.736.
[14] A.S. Ingason, A. Petruhins, M. Dahlqvist, F. Magnus, A. Mockute, B. Alling, et al., A nanolaminated magnetic phase: Mn 2 GaC, Mater. Res. Lett. 2 (2014) 89–93, https://doi.org/10.1080/21663831.2013.865105.
[15] P. Grünberg, R. Schreiber, Y. Pang, M.B. Brodsky, H. Sowers, Layered magnetic structures: evidence for antiferromagnetic coupling of Fe layers across Cr interlayers, Phys. Rev. Lett. 57 (1986) 2442–2445, https://doi.org/10.1103/PhysRevLett.57.2442.
[16] G. Binasch, P. Grünberg, F. Saurenbach, W. Zinn, Enhanced magnetoresistance in layered magnetic structures with antiferromagnetic interlayer exchange, Phys. Rev. B. 39 (1989) 4828–4830, https://doi.org/10.1103/PhysRevB.39.4828.
[17] M.-H. Phan, S.-C. Yu, Review of the magnetocaloric effect in manganite materials, J. Magn. Magn. Mater. 308 (2007) 325–340, https://doi.org/10.1016/j.jmmm.2006.07.025.
[18] X. Moya, L.E. Hueso, F. Maccherozzi, A.I. Tovstolytkin, D.I. Podyalovskii, C. Ducati, et al., Giant and reversible extrinsic magnetocaloric effects in La0.7Ca0.3MnO3 films due to strain, Nat. Mater. 12 (2013) 52–58, https://doi.org/10.1038/nmat3463.
[19] T. Tohei, H. Wada, T. Kanomata, Negative magnetocaloric effect at the antiferromagnetic to ferromagnetic transition of Mn3GaC, J. Appl. Phys. 94 (2003) 1800–1802, https://doi.org/10.1063/1.1587265.
[20] Ö. Çakır, M. Acet, M. Farle, A. Senyshyn, Neutron diffraction study of the magnetic-field-induced transition in Mn 3 GaC, J. Appl. Phys. 115 (2014), 043913, https://doi.org/10.1063/1.4862903.
[21] O. Tegus, E. Brück, K.H.J. Buschow, F.R. de Boer, Transition-metal-based magnetic refrigerants for room-temperature applications, Nature 415 (2002) 150–152, https://doi.org/10.1038/415150a.
[22] M. Dahlqvist, A.S. Ingason, B. Alling, F. Magnus, A. Thore, A. Petruhins, et al., Magnetically driven anisotropic structural changes in the atomic laminate Mn2GaC, Phys. Rev. B. 93 (2016), 014410, https://doi.org/10.1103/PhysRevB.93.014410.
[23] I.P. Novoselova, A. Petruhins, U. Wiedwald, Á.S. Ingason, T. Hase, F. Magnus, et al., Large uniaxial magnetostriction with sign inversion at the first order phase transition in the nanolaminated Mn2GaC MAX phase, Sci. Rep. 8 (2018) 2637, https://doi.org/10.1038/s41598-018-20903-2.
[24] A.S. Ingason, G.K. Palsson, M. Dahlqvist, J. Rosen, Long-range antiferromagnetic order in epitaxial Mn2GaC thin films from neutron reflectometry, Phys. Rev. B 94 (2016), 024416, https://doi.org/10.1103/PhysRevB.94.024416.
[25] X. Zhang, T. He, W. Meng, L. Jin, Y. Li, X. Dai, et al., Mn2C monolayer: hydrogenation/oxygenation-induced strong ferromagnetism and potential applications, J. Phys. Chem. C. 123 (2019) 16388–16392, https://doi.org/10.1021/acs.jpcc.9b04445.
[26] A. Thore, M. Dahlqvist, B. Alling, J. Rosén, First-principles calculations of the electronic, vibrational, and elastic properties of the magnetic laminate Mn 2 GaC, J. Appl. Phys. 116 (2014), 103511, https://doi.org/10.1063/1.4894411.
[27] A.M. Nazmul, H. Shimizu, M. Tanaka, Magneto-optical spectra of epitaxial ferromagnetic MnAs films grown on Si and GaAs substrates, J. Appl. Phys. 87 (2000) 6791–6793, https://doi.org/10.1063/1.372843.
[28] K. Ando, Magneto-optical studies of s, p–d exchange interactions in GaN: Mn with room-temperature ferromagnetism, Appl. Phys. Lett. 82 (2003) 100–102, https://doi.org/10.1063/1.1534618.
[29] A. Petruhins, A.S. Ingason, M. Dahlqvist, A. Mockute, M. Junaid, J. Birch, et al., Phase stability of Cr n+ 1 GaC n MAX phases from first principles and Cr 2 GaC thin-film synthesis using magnetron sputtering from elemental targets, Phys. Status

Solidi – Rapid Res. Lett. 7 (2013) 971–974, https://doi.org/10.1002/pssr.201308025.
[30] A.S. Ingason, A. Petruhins, J. Rosen, Toward structural optimization of MAX phases as epitaxial thin films, Mater. Res. Lett. 4 (2016) 152–160, https://doi.org/10.1080/21663831.2016.1157525.
[31] D.V. Shevtsov, S.A. Lyaschenko, S.N. Varnakov, An ultrahigh-vacuum multifunctional apparatus for synthesis and in situ investigation of low-dimensional structures by spectral magnetoellipsometry in the temperature range of 85–900 K, Instruments Exp. Tech. 60 (2017) 759–763, https://doi.org/10.1134/S0020441217050086.
[32] K. Mok, N. Du, H. Schmidt, Vector-magneto-optical generalized ellipsometry, Rev. Sci. Instrum. 82 (2011), 033112, https://doi.org/10.1063/1.3568822.
[33] O.A. Maximova, S.A. Lyaschenko, M.A. Vysotin, I.A. Tarasov, I.A. Yakovlev, D. V. Shevtsov, et al., Experimental and theoretical in situ spectral magneto-ellipsometry study of layered ferromagnetic structures, JETP Lett. 110 (2019) 166–172, https://doi.org/10.1134/S0021364019150098.
[34] O.A. Maximova, N.N. Kosyrev, S.N. Varnakov, S.A. Lyaschenko, I.A. Yakovlev, I. A. Tarasov, et al., In situ magneto-optical ellipsometry data analysis for films growth control, J. Magn. Magn. Mater. 440 (2017) 196–198, https://doi.org/10.1016/j.jmmm.2016.12.050.
[35] H. Fujiwara, Spectroscopic Ellipsometry Principles and Applications, John Wiley & Sons Ltd, he Atrium, Southern Gate, Chichester, n.d. (2007), P. 388.
[36] H.H. Ku, Notes on the use of propagation of error formulas, J. Res. Nat. Bur. Stand. 70C (4) (1966) 262, https://doi.org/10.6028/jres.070c.025.
[37] S.A. Lyashchenko, Z.I. Popov, S.N. Varnakov, E.A. Popov, M.S. Molokeev, I. A. Yakovlev, et al., Analysis of optical and magnetooptical spectra of Fe5Si3 and Fe3Si magnetic silicides using spectral magnetoellipsometry, J. Exp. Theor. Phys. 120 (2015) 886–893, https://doi.org/10.1134/S1063776115050155.
[38] A. Tillmanns, S. Oertker, B. Beschoten, G. Güntherodt, C. Leighton, I.K. Schuller, J. Nogués, Magneto-optical study of magnetization reversal asymmetry in exchange bias, Appl. Phys. Lett. 89 (2006), 202512, https://doi.org/10.1063/1.2392283.
[39] T.E. Tiwald, D.W. Thompson, J.A. Woollam, W. Paulson, R. Hance, Application of IR variable angle spectroscopic ellipsometry to the determination of free carrier concentration depth profiles, Thin Solid Films 313–314 (1998) 661–666, https://doi.org/10.1016/S0040-6090(97)00973-5.